ASIAN JOURNAL OF CHEMISTRY

Synthesis, Characterization, Thermal Stability and Decomposition Mechanism of [Ru(C₁₂H₈N₂)₃](C₄H₂O₄)(C₄H₃O₄)(C₄H₄O₄)·4H₂O

MIAO SHUI[*], JIE SHU, RONGSHENG LI, YUE SONG, YUANLONG REN and QINGCHUN WANG

The State Key Laboratory Base of Novel Functional Materials and Preparation Science, Faculty of Materials Science and Chemical Engineering, Ningbo 315211, P.R. China

*Corresponding author: Fax: +86 574 87600734; Tel: +86 574 87600147; E-mail: shuimiao@nbu.edu.cn

A new type of Ru(III) complex [Ru(C₁₂H₈N₂)₃](C₄H₂O₄)(C₄H₃O₄)(C₄H₄O₄)·4H₂O is synthesized and characterized. Single-crystal X-ray diffraction shows that the complex belongs to triclinic system, space group P-1, M_r =1058.94 and the cell parameters are a = 12.057(2) Å, b = 12.450(3) Å, c =17.110(3) Å, α = 76.95(3)°, β = 89.87(3)°, γ = 63.82(3)°, V = 2231.5(8) Å³, Z = 2, D_c = 1.576 g/cm³, F(000) = 1086. The thermal stability and decomposition behaviour of the complex is intensively investigated by the method of masterplot, Coats and Redfern and Achar, Brindley and Sharp.

Key Words: Masterplot, Ru(III) complex, Crystal structure, Thermal analysis.

INTRODUCTION

Ru(III) complexes are recently reported to be one of the most promising antitumor drugs because of the following several properties: (a) the ability of ruthenium compounds to specifically accumulate in cancer tissues, in other word, their low toxic to human body; (b) the ability of ruthenium to *mimic* iron in binding to certain biological molecules[1]. Early in 1997, the European Union has established COST D8, a framework for scientific and technical cooperation from all over the world especially centered on the research and development of metal based drugs (including ruthenium) in medical practice. Now, some Ru(II) and Ru(III) based complexes have entered clinical use[2-5]. To further lower the cytotoxicity and improve the therapeutic effects, anticancer drugs are expected to be delivered in the form of nuclear shell structure and restrain the cancer cells in combination with other methods like radiotherapy bringing much heat[6]. Moreover, ruthenium complex is also a promising candidate material for molecular wire, molecular switch, non-linear optical/magnetic devices[7]. Therefore, thermal stability poses challenge for ruthenium based complexes to be applied in those applications.

In this article, a new type of Ru(III) complex [Ru(C₁₂H₈N₂)₃]-(C₄H₂O₄)(C₄H₃O₄)(C₄H₄O₄)·4H₂O is synthesized. The thermal stability and decomposition kinetics of the complex are studied in detail.

EXPERIMENTAL

Synthesis of the ruthenium(III) complex: All chemicals of A.R. grade were commercially available and used without further purification. 8.450 mmol *trans*-butene dioic acid was added slowly into a stirred aqueous solution of RuCl₃·3H₂O (0.13483 g, 0.650 mmol) in 20 mL distilled water until the fumaric acid was dissolved completely. Addition of another 1.95 mmol 1,10-phenanthroline monohydrate into the above mixture produced a dark green solution with black precipitation. After filtration the dark green filtrate was allowed to stand for room temperature. Slow evaporation for 6 weeks afforded violet crystals in the mixture of green amorphous matters at the bottom of the beak with a yield of 15.56 % based on the initial RuCl₃·3H₂O input.

Crystal structure determination: Suitable single crystals were selected under a polarizing microscope and fixed with epoxy cement on respective fine glass fibers which were then mounted on a Rigaku R-axis rapid diffractometer with graphite-monochromated MoKα radiation (λ = 0.71073 Å) for cell determination and subsequent data collection. The reflection intensities for the present ruthenium(III) complex were collected at 293 K using θ-2θ scan technique with 2θ range between 6° and 55°. There were overall 22030 data points collected. All the collected data were corrected for LP and absorption effects. SHELXS-97 and SHELXL-97 programs[8]

TABLE-1
SUMMARY OF CRYSTAL DATA, DATA COLLECTION, STRUCTURE SOLUTION AND
REFINEMENT DETAILS FOR THE TITLE COMPLEX

Empirical formula	$C_{48}H_{41}N_6O_{16}Ru$	λ [MoK$_\alpha$] (Å)	0.71073
Molecular weight	1058.94	Monochromator	Graphite monochromator
Description	Violet block	Scanning mode	Plane detector scanning
Crystal system	Triclinic crystal simple crystal	Diffraction point number and angle range	22030, 6º ≤ 2θ ≤ 55º
Space group	P-1	Diffraction indices range	-15<=h<=15, -15<=k<=16, -22<=l<=22
a (Å) b (Å) c (Å)	12.058(2) 12.450(3) 17.110(3)	Independent reflections	10095
α (°) β (°) γ (°)	76.95(3) 89.87(3) 63.82(3)	Number of parameters	640
V [Å³]	2231.6(8)	R_{int}	0.0213
Z	2	R_{sigma}	0.0298
D_c (g cm⁻³)	1.576	wR (F²), R (|F$_o$|)	0.1135, 0.0397
F(000)	1086	wR (F²), R (|F$_o$|) (F² ≥ 2σ (F$_o$²))	0.1177, 0.0457
Crystal appearance	Bulk	w	w = [σ²(F$_o$²) + (0.1000P)²]⁻¹
Crystal size (mm)	0.311 × 0.222 × 0.089	p	P = [Max(F$_o$², 0) + 2F$_c$²]/3
Diffractometer	R-Axis Rapid	Goodness	1.077
T (K)	293(2)	δρ$_{max}$, δρ$_{min}$ (e Å⁻³)	1.538, -1.066

were used for structure solution and refinement. The structures were solved by using direct methods. Subsequent difference Fourier syntheses enabled all non-hydrogen atoms to be located. All hydrogen atoms associated with carbon atoms were geometrically generated. Finally, all non-hydrogen atoms were refined with anisotropic displacement parameters by the full-matrix least-squares technique and hydrogen atoms were refined with isotropic displacement parameters. Detailed information about the crystal data and structure determination is summarized in Table-1.

Decomposition kinetics: The commonly used equation in the non-isothermal decomposition kinetics is presented below:

$$\frac{d\alpha}{dt} = kf(\alpha) \tag{1}$$

where the kinetic function f(α) is determined by reaction mechanism and speed controlling step. It has another form as:

$$g(\alpha) = \int_0^\alpha \frac{d\alpha}{f(\alpha)} \tag{2}$$

where g(α) is an another form of kinetic function. The commonly used fifteen kinetic functions were proposed by Dollimors *et al.*[9].

Since the mechanism determination and the kinetic parameter calculation are mutually dependent, non-mechanism equation is firstly introduced to estimate the activation energy as a prerequisite for determining the reaction mechanism. After the reaction mechanism is deduced, mechanism equations are then used to further confirm the kinetic parameters obtained previously. Freeman-Carroll[10] equation and Kissinger[11] equation are commonly used non-mechanism equations. However, there is evidence that the former may yield diffusive data points. So, Kissinger equation:

$$\ln(A) = \ln(\frac{Ea}{R}) - \ln(\frac{T_p^2}{\beta}) + \frac{Ea}{RT_p} \tag{3}$$

is applied to estimate the activation energy where T_p represents the peak temperature of DTA curve, β is the heating rate. Although some authors suggested that T_m, peak temperature

of DTG curve, rather than T_p should be used in the above formula, T_p is still preferred when the reaction proceeds over narrow temperature range (between 0.9 T_m-1.1 T_m). In this case, T_p is close to T_m and easy to be accurately determined.

In the mechanism determining process, methods proposed by Berggern and Satava[12] (plot log(g(α)) against 1/T) and by Coats and Redfern[13] (plot log(g(α)/T²) against 1/T) are not sensitive enough to distinguish some mechanisms. Master plot method[14] less influenced by experimental conditions is used to determine the reaction mechanism. That is, plot z(α) = f(α) × g(α) against a for all possible mechanisms and thus establish a series of standard curves. The curve that best fits the experimental data in the form of

$$z(\alpha) = \frac{d\alpha/dt}{\beta} \cdot \pi(x) \cdot T \tag{4}$$

where $\pi(x) = \dfrac{x^3 + 18x^2 + 88x + 96}{x^4 + 20x^3 + 120x^2 + 240x + 120}$ $x = \dfrac{Ea}{RT}$ β represents the heating rate, should be considered as the reaction mechanism.

Afterwards, Achar, Brindley and Sharp equation[15], referred to as differential method:

$$\ln(\frac{1}{f(\alpha)}\frac{d\alpha}{dT}) = \ln(\frac{A}{\beta}) + \frac{Ea}{RT} \tag{5}$$

and Coats and Redfern equation[13], referred to as integral method:

$$\log(\frac{g(\alpha)}{T^2}) = \log(\frac{AR}{E\beta}) - \frac{Ea}{2.303RT} \tag{6}$$

are further used to confirm the obtained activation energy and kinetic mechanism.

RESULTS AND DISCUSSION

Description of crystal structures: Atomic parameters and equivalent isotropic thermal parameters of selected non-hydrogen atoms are listed in Table-2. Anisotropic thermal parameters of selected non-hydrogen atoms for the title complex are listed in Table-3. Fig. 1 shows the ORTEP view of coordination environments of ruthenium atoms. Fig. 2 shows

TABLE-2
ATOMIC PARAMETERS AND EQUIVALENT ISOTROPIC THERMAL PARAMETERS OF
SELECTED NON-HYDROGEN ATOMS FOR THE Ru(III) COMPLEX

Atom	x	y	z	$U_{eq}[\text{Å}^2]$	Atom	x	y	z	$U_{eq}[\text{Å}^2]$
Ru	0.1899(0)	0.3286(0)	0.7696(0)	0.02279(7)	C(1)	0.4618(3)	0.2486(3)	0.8288(2)	0.0373(6)
N(1)	0.3789(2)	0.2202(2)	0.7985(1)	0.0289(4)	C(2)	0.5887(3)	0.1705(3)	0.8379(2)	0.0467(8)
N(2)	0.2101(2)	0.1707(2)	0.7377(1)	0.0271(4)	O(1)	0.6303(3)	0.0781(3)	1.0675(2)	0.0669(7)
N(3)	0.2090(2)	0.4034(2)	0.6527(1)	0.0273(4)	O(2)	0.4382(3)	0.2278(3)	1.0456(2)	0.0708(8)
N(4)	0.0054(2)	0.4460(2)	0.7256(1)	0.0267(4)	O(3)	-0.4260(2)	1.1415(2)	0.5845(2)	0.0625(7)
N(5)	0.1885(2)	0.4685(2)	0.8167(1)	0.0281(4)	O(4)	-0.2972(3)	0.9504(3)	0.5797(2)	0.0757(9)
N(6)	0.1556(2)	0.2731(2)	0.8864(1)	0.0373(6)	O(5)	-0.2452(2)	0.1350(2)	0.6606(2)	0.0589(6)

TABLE-3
ANISOTROPIC THERMAL PARAMETERS OF SELECTED NON-HYDROGEN ATOMS FOR THE Ru(III) COMPLEX ($\text{Å}^2 \times 10^3$)

Atom	U_{11}	U_{22}	U_{33}	U_{12}	U_{13}	U_{23}
Ru	0.02204(11)	0.02236(11)	0.02260(11)	-0.00913(8)	0.00240(7)	-0.00506(7)
N(1)	0.0248(10)	0.0293(10)	0.0282(10)	-0.0112(9)	0.0020(8)	-0.0015(8)
N(5)	0.0269(10)	0.0257(10)	0.031(1)	-0.0115(9)	0.0018(8)	-0.0066(8)
C(13)	0.0293(13)	0.0411(14)	0.0343(13)	-0.0152(12)	0.0070(11)	-0.0081(11)
C(18)	0.0466(18)	0.0325(15)	0.0400(16)	-0.0014(13)	-0.0090(14)	0.0002(12)
O(1)	0.0458(14)	0.0665(17)	0.085(2)	-0.0200(13)	-0.0006(14)	-0.0237(15)
O(2)	0.0578(16)	0.0656(17)	0.0793(19)	-0.0122(14)	-0.0100(14)	-0.0329(15)
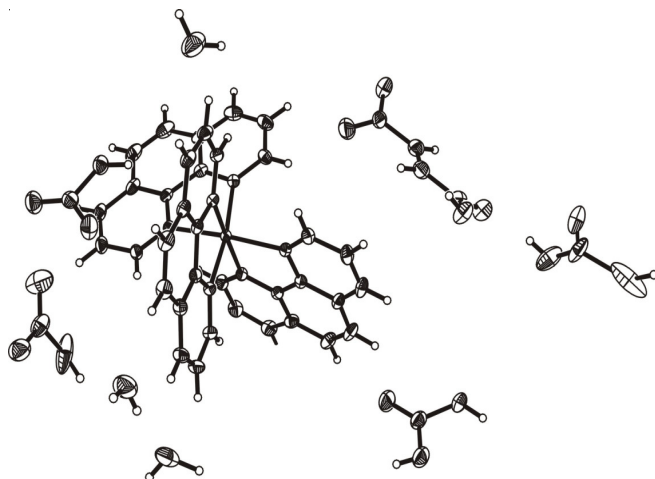
Fig. 1.   ORTEP view of coordination environments of Ru atoms in the present complex

the stacking diagram of the present Ru(III) complex along axis a. The unit cell contains one Ru(III) cation, 3 phenanthroline molecules, 3 ionized fumaric acid molecules and 4 water molecules. The Ru atoms are each octahedrally coordinated by two N atoms of phenanthroline molecule. The bond angles of N-Ru-N fall in the region 173.65(8)° -79.53(9)° exhibiting slight deviation from the corresponding normal values of a regular octahedron. Carbonic rings in phenanthroline molecule are slightly twisted. Such configuration stabilizes the molecule. The Ru-N bond distances fall in the range 2.027-2.108 Å. Four fumaric acid molecules are shared by two adjacent unit cells. Therefore averagely, there are 3 fumaric acid molecules in one unit cell to counter balance the positive charge of the central metal ion. Interestingly, 3 fumaric acid molecules exist with one carboxyl group ionized, two carboxyl groups ionized and carboxyl without ionization, respectively. The oxygen atoms in fumaric acid also bind the neighboring H atom on carbonic ring of phenanthroline molecules or in water molecules by hydrogen bond. Within the crystal structure,

the trivalent complex cations are arranged so that the phens of the phenanthroline molecules are aligned face to face and the mean phen-to-phen distance of 3.5 Å indicates strong π-π stacking interactions as indicated by the arrow in Fig. 2.
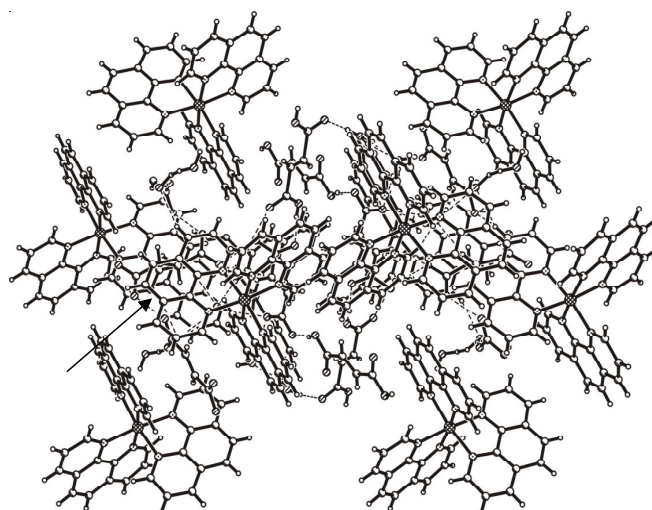
Fig. 2. Stacking diagram of the present Ru(III) complex along axis a

Thermal stability and decomposition kinetics of the present Ru(III) complex: Fig. 3 shows the TG/DTA measurements of the present Ru(III) complex in air atmosphere at the heating rate of 10 K/min. Thermal decomposition of the present Ru(III) complex shows three stages. The first stage stats at room temperature and continues until 200 ºC. 8.4 % weight loss at this stage is supposed to be desorption of the adsorbed water and the water of crystallization. The adsorbed water is calculated to be 1.6 % since the theoretical crystal water percentage of title complex is 6.8 %. In the second stage, the weight of title complex falls quickly with the elevating temperature until temperature reaches 299 ºC. Accompanied by a strong exothermic peak on corresponding DTA curves, this weight loss can reasonably be related to the oxidation of
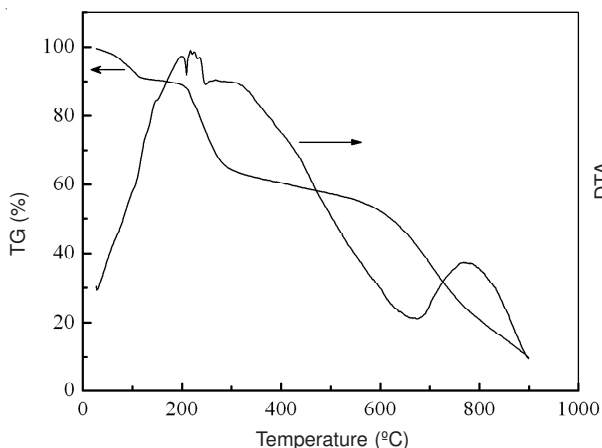
Fig. 3. TG-DTA curves of the Ru(III) complex

fumaric acid in air, which is in good agreement with the theoretical weight percentage of three fumaric acid (those oxygen atoms in fumaric acid molecule associated to ruthenium after the thermal treatment are excluded) in this complex, *ca.* 30.1 %. In the third stage, the present complex loses weight slowly over temperature region 300-576 ℃ where no obvious thermal effect is observed with a weight loss *ca.* 9.2 %. Then over temperature range 580-900 ℃, 43.2 % weight loss appears on TG curve with an endothermic peak at about 680 ℃ and a strong exothermic peak near 800 ℃. The overall weight loss in this stage amounts to 52.4 %, close to the calculated value of 51.2 % for three mole phenanthroline molecules per formula unit. Therefore, the weight loss in this stage can be explained by the breakdown of coordination bond between the ligand and the central ruthenium ion and the oxidation of more stable
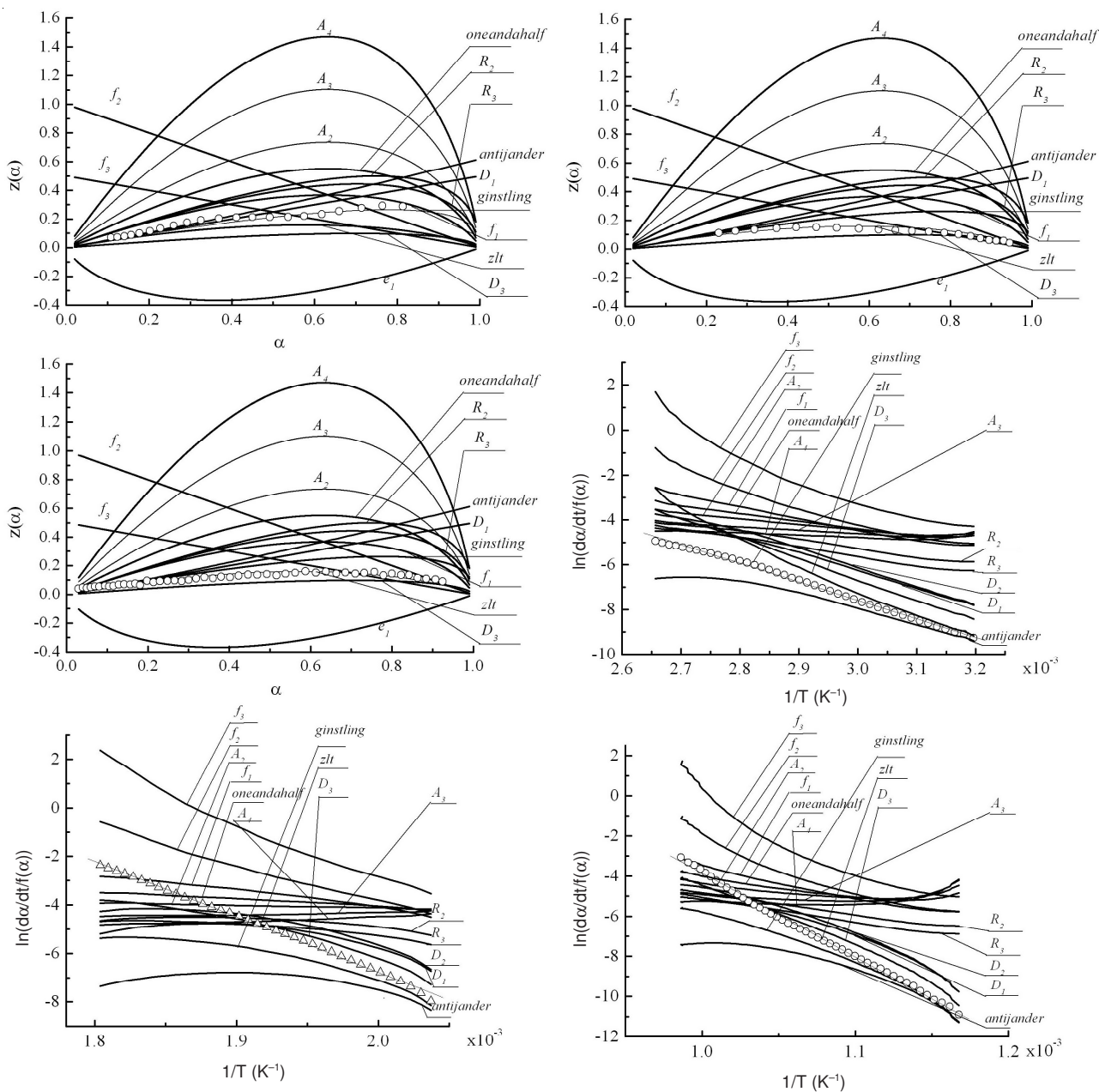
Fig. 4.   Master plot curve of (a) the 1st stage (b) the 2nd stage (c) the 3rd stage and $\ln\left(\dfrac{d\alpha}{f(\alpha)dT}\right)$ *vs.* 1/T in (d) the 1st stage (e) the 2nd stage (f) the 3rd stage for Ru(III) complex

TABLE-4
MECHANISM AND ACTIVATION ENERGY AT VARIOUS THERMAL DECOMPOSITION STAGES

	Mechanism	Heating rate (K/min)	Ea (kJ mol^{-1})	
			Differential method Achar, Brindley and Sharp	Integral method Coats and Redfern
1st stage	Ginstling-Brounshtein	10	76.2	72.2
2nd stage	Zlt	10	210.5	195.3
3rd stage	zlt	10	360.7	351.6

phenanthroline molecules in air. The final residue after heat treatment is supposed to be ruthenium oxide (calc. 11.8 % against obs. 11.9 %).

Decomposition kinetics of the present Ru(III) complex is studied according to the reported methods. Fig. 4 shows the determination of reaction mechanism by masterplot method and the further confirmation of decomposition kinetics according to redfern and coats equation. Ginstling-Brounshtein (three dimensional diffusion mechanism) best matches the experimental data line since vapour diffusion is usually the rate determination step in the process of water desorption in first stage while zlt is the most appropriate mechanism in the other two stages. The calculated $\ln\left(\dfrac{d\alpha}{f(\alpha)dT}\right)$ where f(α) is determined according to masterplot method has better linear relationship with 1/T. The activation energies calculated according to Achar, Brindley and Sharp equation are close to those calculated by Coats and Redfern equation and the results are listed in Table-4. From the table, the increasing average activation energy in three decomposition stages indicates the gradually enhanced interactions between the leaving segment and the remaining part in the complex. The activation energy of the first stage seems much larger than the energy of hydrogen bond (30-40 KJ/mol) possibly because the resistance of H_2O leaving comes mainly from diffusion rather than overcoming hydrogen bond energy.

Conclusion

(1) The synthesized new type of Ru(III) complex [Ru(C$_{12}$H$_8$N$_2$)$_3$](C$_4$H$_2$O$_4$)(C$_4$H$_3$O$_4$)(C$_4$H$_4$O$_4$)·4H$_2$O belongs to triclinic system, space group P-1, M$_r$ = 1058.94 and the cell parameters are a = 12.057(2) Å, b = 12.450(3) Å, c = 17.110(3) Å, α = 76.95(3)°, β = 89.87(3)°, γ = 63.82(3)°, V = 2231.5(8) Å^3, Z = 2, D$_c$ = 1.576 g/cm^3, F(000) = 1086.

(2) This new type of Ru(III) complex decomposes according to Ginstling-Brounshtein mechanism in first stage and zlt for the other two stages. The average activation energies of three stages are 76.2 kJ mol^{-1}, 210.5 kJ mol^{-1} and 360.7 kJ mol^{-1}, respectively. Masterplot method, Coats and Redfern equation, Achar, Brindley and Sharp equation are applied here comprehensively to determine accurate and reliable decomposition kinetics.

REFERENCES

1. S.C. Srivastava, P. Richard, G.E. Meinken, S.M. Larson, Z. Grunbaum, R.P. Spencer, Tumor Uptake of Radioruthenium Compounds. In: Radiopharmaceuticals Structure-Activity Relationships, Grune & Stratton Inc.: New York, p. 207 (1981).
2. Y.N.V. Gopal, N. Konuru and A.K. Kondapi, *Arch. Biochem. Biophys.*, **401**, 53 (2002).
3. G. Sava, A. Bergamo, S. Zorzet, B. Gava, C. Casarsa, M. Cocchietto, A. Furlani, V. Scarcia, B. Serli, E. Iengo, E. Alessio and G. Mestroni, *Eur. J. Cancer*, **38**, 427 (2002).
4. B. Serli, E. Iengo, T. Gianferrara, E. Zangrando and E. Alessio, *Metal Based Drugs*, **8**, 9 (2001).
5. B. Serli, E. Zangrando, E. Iengo and E. Alessio, *Inorg. Chim. Acta*, **339**, 265 (2002).
6. M.D. Green, C.D. King, B. Mojarrabi, P.I. Mackenzie and T.R. Tephly *Drug. Metab. Dispos.*, **26**, 507 (1998).
7. W.Z. Wang, D.Z. Liao and G.L. Wang, *Huaxue Tongbao*, **2**, 107 (2002).
8. SHELXTL Version 5.1 Reference Manual, Siemens Analytical X-ray Systems, Inc., Madison, WI, USA (1996).
9. D. Dollimors, P. Tong and K. Alexander, *Thermochim. Acta*, **282/283**, 13 (1996).
10. E.S. Freeman and B. Carroll, *J. Phys. Chem.*, **62**, 394 (1958).
11. H.E. Kissinger, *J. Res. Notl. Bur. Stand*, **57**, 712 (1956).
12. V. Satava, *Thermochim. Acta*, **2**, 423 (1971).
13. A.W. Coats and J.P. Redfern, *Nature*, **201**, 68 (1964).
14. J. Malek, *Thermochim. Acta*, **200**, 257 (1992).
15. J.H. Sharp and S.A. Wendworth, *Anal. Chem.*, **41**, 2060 (1969).